

## Synthesis and Quantum Chemical Calculations of 4-(2-Fluorophenyl)-1-(2-oxoindolin-3-ylidene)thiosemicarbazone and its Zinc(II) Complex

F. KANDEMIRLI<sup>1,\*</sup>, Y. AKKAYA<sup>2</sup> and C.D. VURDU<sup>1</sup><sup>1</sup>Biomedical Engineering Department, Faculty of Engineering and Architecture, Kastamonu University, Kastamonu, Turkey<sup>2</sup>Department of Chemistry, Faculty of Science, Nigde University, Nigde, Turkey

\*Corresponding author: Fax: +90 366 2154969; Tel: +90 366 2801908; E-mail: fkandemirli@yahoo.com

(Received: 28 January 2013;

Accepted: 18 October 2013)

AJC-14262

In this study, wavenumbers, IR intensities and molecular parameters of 4-(2-fluorophenyl)-1-(2-oxoindolin-3-ylidene)thiosemicarbazone ( $I_2\text{FPTH}_2$ ) and its zinc(II) complex have been studied theoretically by using the *ab initio* Hartree-Fock (HF) method with the 3-21G, 3-21G\*, 6-31G(d,p), 6-311G (d,p), 6-311++G (d,p) and 6-311++G (2d,2p) basis sets. In addition to theoretical study, they have been prepared for characterization of structure by means of elemental analyses which are FT-IR, electronic and  $^1\text{H}$  NMR Zn(II) complex spectra. Moreover, according to the results of Fukui functions values of  $I_2\text{FPTH}_2$ , calculated with B3LYP/6-31G(d,p) and B3LYP/6-311G(d,p), the contribution of sulphur to the HOMO is found predominant 47.69 and 49.16 %, respectively while the contribution of nitrogen to the LUMO is also found dominant as 24.82 and 24.21 %, respectively. The theoretical results of wavelengths,  $^1\text{H}$  and  $^{13}\text{C}$  NMR for wavenumbers are sensibly consistent with the results of experimental study.

**Key Words:** Thiosemicarbazone, DFT,  $^1\text{H}$  NMR,  $^{13}\text{C}$  NMR, FT-IR spectra.

### INTRODUCTION

Isatin (1*H*-indole-2,3-dione) is one of the endogenous compounds, which possess a wide range of biological activities. It has been also reported for derivatives of 4-(2-fluorophenyl)-1-(2-oxoindolin-3-ylidene)thiosemicarbazone ( $I_2\text{FPTH}_2$ ) that results have been found considerable attention, because of variable bonding abilities and antiviral, antibacterial, anti-tumor and antifungal activity and inhibitory action<sup>1-9</sup>. Isatin thiosemicarbazones have been known to be certain of their coordination compounds.

Several isatin thiosemicarbazones and Zn(II) to Ni(II) complexes were previously studied theoretically and synthesized experimentally<sup>8,10-13</sup>. In the literature, the crystal structure of 4-(2-fluorophenyl)-1-(2-oxoindolin-3-ylidene)thiosemicarbazone ( $I_2\text{FPTH}_2$ ) were reported<sup>14</sup>, but there are no theoretical study about it and also no synthesis of Zn(II) complex of  $I_2\text{FPTH}_2$  ligand.

According to results of the experimental and quantum chemical studies of 5-fluoroisatin-3-N(cyclohexylthiosemicarbazone) and its metal complexes, it was found that only one part of the ligand was coordinated to the metal ion resulting mono-nuclear complexes in Ni(II) and Zn(II) complexes<sup>15</sup>.

In this study, the vibrational spectrum, UV spectrum,  $^{13}\text{C}$  NMR,  $^1\text{H}$  NMR values, the molecular geometry, the atomic

charges and molecular polarizability were carried out for 4-(2-fluorophenyl)-1-(2-oxoindolin-3-ylidene)thiosemicarbazone molecule by using density functional theory (DFT) with B3LYP hybrid functional and *ab initio* Hartree-Fock (HF) computations with the basis sets of 3-21G, 3-21G\*, 6-31G(d,p), 6-311G (d,p), 6-311++G (d,p), 6-311++G (2d,2p)<sup>16</sup>. Fukui functions were also calculated by using AOMix program<sup>17,18</sup> from single-point calculations with B3LYP/6-311G(d,p)<sup>16</sup>.

### EXPERIMENTAL

4-(2-Fluorophenyl)-1-(2-oxoindolin-3-ylidene) thiosemicarbazone molecule was synthesized as reported<sup>18</sup>. The FTIR spectra was recorded using Jasco 300 FTIR spectrometer in the region 4000-200  $\text{cm}^{-1}$ . UV spectra was recorded UV-160A Shimadzu<sup>1</sup>.

**Synthesis of bis[4-(2-fluorophenyl)thiosemicarbazonato]zinc(II) complex  $\text{Zn}[(I_2\text{FPTH})_2]$ :** 1 mmol (0.3142 g)  $I_2\text{FPTH}_2$  was dissolved in 20 mL of ethanol at 50-55 °C, before they were slowly added an ethanol solution (10 mL) of 0.5 mmol (0.1097 g) zinc acetate tetrahydrate. The mixture was refluxed for 6-9 h at a temperature of approximately. Light orange product was precipitated during the reaction and then it was washed with ethanol and diethyl ether. Finally, it was dried (m.p. 238 °C). (calculated: (%) C: 51.66, H: 2.92, N:

15.91, S: 8.98, found (%): C: 51.206, H: 2.97, N: 15.22, S: 8.25).

**Computational methodology:** Theoretical calculations which are vibrational, wavenumbers, geometric parameters, atomic charges and the other molecular properties were performed by using the GAUSSIAN 09 package program<sup>16</sup>. Both ab initio calculations and DFT calculations were carried out by using B3LYP with basis sets of 3-21G, 3-21G\*, 6-31G(d,p), 6-311G (d,p), 6-311++G (d,p), 6-311++G (2d,2p). The harmonic unscaled vibrational frequencies were calculated for every each completely optimized geometry by analytical differentiation algorithms. Fukui functions were also calculated from results of single-point calculations with B3LYP/6-311G(d,p) by using AOMix<sup>17,18</sup>.

## RESULTS AND DISCUSSION

**Geometric parameters:** Crystallographic studies of 4-(2-fluorophenyl)-1-(2-oxoindolin-3-ylidene)thiosemicarbazone molecule show that molecules form inversion dimers in the crystal<sup>14</sup>. Therefore, the experimental X-ray data of 4-(2-fluorophenyl)-1-(2-oxoindolin-3-ylidene)thiosemicarbazone is used to calculate geometrical parameters. The conformation is stabilized by intramolecular N-H---N and N-H---O hydrogen bonds which generate S and the other S rings, respectively<sup>14</sup>. N-H---F and C-H---S interactions. The X-ray structure of 4-(2-fluorophenyl)-1-(2-oxoindolin-3-ylidene)-thiosemicarbazone dimer is shown in Fig. 1. The labeling of the atoms in the monomer form by using DFT method at the B3LYP/6-31G(d) level is also shown in Fig. 2.

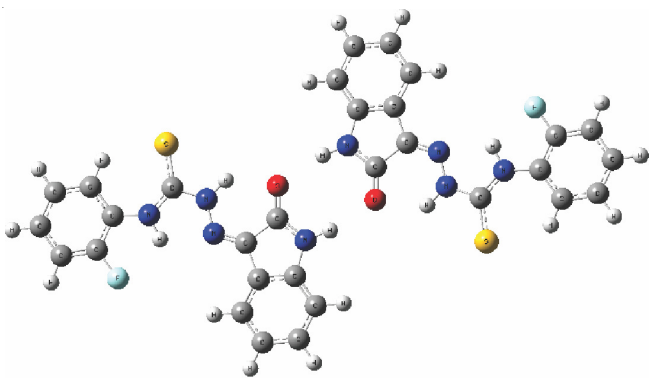


Fig. 1. Geometry of 4-(2-fluorophenyl)-1-(2-oxoindolin-3-ylidene)thiosemicarbazone dimer optimized at the B3LYP/6-311++G(2d,2p) level

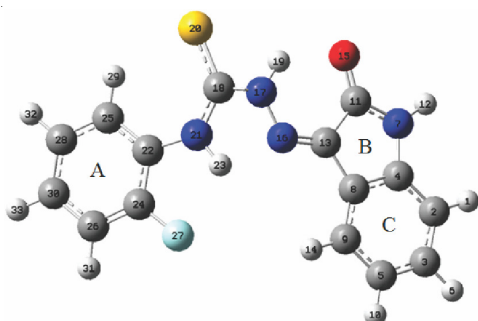


Fig. 2. Geometry of 4-(2-fluorophenyl)-1-(2-oxoindolin-3-ylidene)thiosemicarbazone calculated single point energy with the B3LYP/6-311++G(2d,2p) level

The optimized geometrical parameters, calculated by using the density functional and RHF methods, with the experimental data are summarized for studied molecule in Table-1. Calculated bond lengths are found systematically longer than experimental result. A statistical treatment of these data (see at the bottom of Table-1) shows that RHF for the bond lengths is slightly better than the B3LYP for all calculated basis sets. The highest correlation coefficient for bond lengths is 0.9745 for RHF/6-311++ G(2d,2p).

The crystal structure of I2FPTH<sub>2</sub> was studied by Pervez *et al.*<sup>14</sup>. Experimental bond lengths of C28-C30, C30-C26, C26-C24 and C24-C22 belonging to phenyl group are 1.351, 1.368, 1.373 and 1.370 Å while their theoretical bond lengths calculated by B3LYP/6-311++ G(2d,2p) are 1.389, 1.393, 1.376 and 1.400 Å, respectively. Moreover, experimental bond lengths of C18-S20, C18-N17, N17-N16, N16-C13 belonging to thiosemicarbazone group are 1.635, 1.378, 1.344 and 1.291 Å, respectively while their theoretical bond lengths calculated by B3LYP/6-311++ G(2d,2p) are 1.666, 1.390, 1.332 and 1.293 Å, respectively.

Some of the experimental and theoretical bond angles (°) values calculated by using B3LYP and RHF method for 4-(2-fluorophenyl)-1-(2-oxoindolin-3-ylidene)thiosemicarbazone are summarized in Table-2. The correlation coefficients were calculated in 0.979, 0.979, 0.989, 0.984, 0.982, 0.979 and 0.990 for bond angles by using B3LYP. Besides, the correlation coefficients are 0.973, 0.980, 0.978, 0.978, 0.970, 0.979 and 0.979 for RHF with basis sets of 3-21G, 3-21G\*, 6-31G(d,p), 6-311G(d,p), 6-311+G(d,p), 6-311++G(d,p) and 6-311++G(2d,2p), respectively. The agreement between the calculated and the experimental bond angles is better than for the bond lengths.

The Mullikan and NBO charge values calculated with B3LYP and RHF methods are given in Table-3. Mullikan charges calculated with RHF/6-311G(d,p) predict a much more positive charge and negative charges on atoms for I2FPTH<sub>2</sub>, except C3 and C28 atoms, as seen in Table-3. It is resulted from NBO analysis that O15 atom has the largest negative charge in the indole ring and N21 has the largest negative charge in the thiosemicarbazone group.

Values of Fukui functions calculated with B3LYP/6-31G(d,p) and B3LYP/6-311G(d,p) were summarized for I2FPTH<sub>2</sub> in Table-4. The contributions of S20, N17 and N21 atoms to the HOMO are calculated with B3LYP/6-311G(d,p) as 47.69, 6.74 and 6.31 %, respectively, while they are calculated as 49.16, 5.03 and 8.35 % by using B3LYP/6-31G(d,p), respectively. Moreover, the contributions of C11, C13, O15, N16, S20 and N21 atoms to the LUMO are 9.88, 13.73, 8.27, 24.21, 8.58 and 1.72 % in calculations done by B3LYP/6-311G(d,p), respectively while they are 9.99, 13.41, 8.71, 24.82, 8.34 and 1.81 % in calculations carried out by B3LYP/6-31G(d,p), respectively.

**IR studies:** The IR spectra of solid I2FPTH<sub>2</sub> and Zn[(I2FPTH)<sub>2</sub>] are shown in Fig. 3(a-c). The B3LYP/6-311G(d,p) calculations were used to obtain computed harmonic vibrational frequencies and infrared intensities for I2FPTH<sub>2</sub> and Zn[(I2FPTH)<sub>2</sub>]. Table-5 lists theoretical and experimental bands of the IR spectra of the I2FPTH<sub>2</sub> and Zn[(I2FPTH)<sub>2</sub>] in the 4000-1250 cm<sup>-1</sup> spectral region.

TABLE-1  
SELECTED EXPERIMENTAL AND THEORETICAL BOND LENGTHS (Å) THEORETICAL VALUES CALCULATED BY (A)  
B3LYP AND (B) RHF METHOD FOR 4-(2-FLUOROPHENYL)-1-(2-OXOINDOLIN-3-YLIDENE)THIOSEMICARBAZONE

Atoms	Exp.	(a) B3LYP						
		3-21G	3-21G*	6-31 G(d,p)	6-311 G(d,p)	6-311+ G(d,p)	6-311++ G(d,p)	6-311++ G(2d,2p)
Bond lengths (Å)								
C28-C30	1.351	1.395	1.395	1.394	1.391	1.392	1.392	1.389
C30-C26	1.368	1.398	1.398	1.397	1.395	1.395	1.395	1.393
C26-C24	1.373	1.379	1.379	1.381	1.378	1.378	1.378	1.376
C24-F27	1.365	1.383	1.383	1.361	1.362	1.364	1.365	1.362
C24-C22	1.370	1.405	1.405	1.405	1.403	1.403	1.403	1.400
C22-N21	1.407	1.403	1.403	1.403	1.403	1.403	1.403	1.402
N21-C18	1.343	1.348	1.348	1.353	1.352	1.354	1.354	1.351
C18-S20	1.635	1.719	1.719	1.672	1.670	1.668	1.668	1.666
C18-N17	1.378	1.390	1.390	1.393	1.393	1.394	1.394	1.390
N17-N16	1.344	1.376	1.376	1.336	1.333	1.333	1.333	1.332
N16-C13	1.291	1.301	1.301	1.299	1.295	1.295	1.295	1.293
C13-C11	1.498	1.501	1.501	1.500	1.502	1.501	1.501	1.500
C11-O15	1.229	1.259	1.259	1.240	1.233	1.235	1.235	1.234
C11-N7	1.348	1.370	1.370	1.365	1.363	1.363	1.363	1.362
N7-C4	1.406	1.413	1.413	1.408	1.407	1.407	1.407	1.406
C4-C2	1.367	1.385	1.385	1.387	1.385	1.385	1.385	1.382
C2-C3	1.376	1.403	1.403	1.401	1.399	1.399	1.399	1.397
C3-C5	1.377	1.400	1.400	1.399	1.397	1.398	1.397	1.395
C5-C9	1.377	1.400	1.400	1.398	1.395	1.396	1.396	1.393
C9-C8	1.387	1.390	1.390	1.393	1.391	1.391	1.391	1.389
C8-C4	1.381	1.416	1.416	1.412	1.409	1.409	1.409	1.407
C13-C8	1.445	1.455	1.455	1.456	1.455	1.456	1.456	1.454
C22-C25	1.375	1.399	1.399	1.401	1.399	1.400	1.400	1.397
C25-C28	1.377	1.397	1.397	1.397	1.394	1.394	1.394	1.391
R <sup>2</sup>	0.9567	0.9567	0.9684	0.9721	0.9724	0.9724	0.9724	0.9738
(b) RHF								
C28-C30	1.351	1.394	1.381	1.380	1.381	1.381	1.378	1.389
C30-C26	1.368	1.398	1.387	1.386	1.386	1.386	1.383	1.393
C26-C24	1.373	1.378	1.370	1.369	1.369	1.369	1.367	1.376
C24-F27	1.365	1.383	1.341	1.337	1.336	1.336	1.334	1.362
C24-C22	1.370	1.406	1.391	1.390	1.390	1.390	1.387	1.400
C22-N21	1.407	1.401	1.408	1.408	1.408	1.408	1.406	1.402
N21-C18	1.343	1.355	1.334	1.335	1.336	1.336	1.333	1.351
C18-S20	1.635	1.668	1.675	1.673	1.671	1.671	1.670	1.666
C18-N17	1.378	1.401	1.365	1.364	1.365	1.365	1.361	1.390
N17-N16	1.344	1.373	1.336	1.335	1.335	1.335	1.334	1.332
N16-C13	1.291	1.301	1.260	1.258	1.258	1.258	1.255	1.293
C13-C11	1.498	1.500	1.511	1.514	1.514	1.514	1.512	1.500
C11-O15	1.229	1.260	1.207	1.201	1.202	1.202	1.202	1.234
C11-N7	1.348	1.370	1.345	1.345	1.345	1.345	1.342	1.362
N7-C4	1.406	1.413	1.403	1.403	1.403	1.403	1.402	1.406
C4-C2	1.367	1.385	1.376	1.375	1.376	1.376	1.372	1.382
C2-C3	1.376	1.403	1.391	1.390	1.391	1.391	1.388	1.397
C3-C5	1.377	1.400	1.388	1.387	1.388	1.388	1.385	1.395
C5-C9	1.377	1.400	1.388	1.388	1.388	1.389	1.386	1.393
C9-C8	1.387	1.390	1.380	1.379	1.379	1.379	1.376	1.389
C8-C4	1.381	1.416	1.393	1.391	1.391	1.391	1.388	1.407
C13-C8	1.445	1.455	1.466	1.466	1.467	1.467	1.465	1.454
C22-C25	1.375	1.399	1.387	1.386	1.387	1.387	1.384	1.397
C25-C28	1.377	1.397	1.388	1.388	1.388	1.388	1.385	1.391
R <sup>2</sup>	0.964	0.971	0.9741	0.9744	0.9737	0.9729	0.9745	

The IR spectrum of I<sub>2</sub>FPTH<sub>2</sub> shows that bands at 3313 cm<sup>-1</sup> attributed to v(NH) cm<sup>-1</sup> vibration of the indole ring and thiosemicarbazone moiety. On complex formation, the position of these bands shifted to 3364 cm<sup>-1</sup> due to changes in hydrogen bonding. A strong band at 1690 and 1697 cm<sup>-1</sup> assigned to (C=O) stretching vibration of ligand and its Zn(II) complex, respectively. This indicates that CO group is uncoordinated in its Zn(II) complex.

Abdullah *et al.*<sup>20</sup> reported that all the thiosemicarbazones remain in their thione form due to the existence of a strong band in the region 1038–1026 cm<sup>-1</sup> due to v(C=S) and absence of any band in the region 2600–2500 cm<sup>-1</sup> due to v(C-SH) for steroidal thiosemicarbazones.

The C=S band appearing at 817 cm<sup>-1</sup> in the IR spectrum of I<sub>2</sub>FPTH<sub>2</sub> ligand is shifted towards lower wave number in

TABLE-2  
SELECTED EXPERIMENTAL AND THEORETICAL BOND ANGLES ( $^{\circ}$ ) VALUES  
CALCULATED BY (A) B3LYP AND (b) RHF METHOD FOR I<sub>2</sub>FPTH<sub>2</sub>

Atoms	Exp.	(a) B3LYP						
		3-21G	3-21G*	6-31 G(d,p)	6-311 G(d,p)	6-311+ G(d,p)	6-311++ G(d,p)	6-311++ G(2d,2p)
Bond angles ( $^{\circ}$ )								
C1-C3-F32	120.1	120.7	120.7	119.5	119.3	119.1	119.1	119.1
F32-C3-C13	116.5	116.9	116.9	117.3	119.3	117.5	117.5	117.5
C3-C13-N19	116.8	114.7	114.7	115.4	115.7	117.5	116.0	116.0
C14-C13-N19	126.6	127.2	127.2	127.1	126.9	126.8	126.8	126.8
C13-C3-C1	123.4	122.4	122.4	123.1	123.1	123.4	123.4	123.4
C3-C1-C2	118.1	119.1	119.1	118.6	118.7	118.6	118.6	119.5
C1-C2-C8	120.2	119.5	119.5	119.6	119.5	119.5	119.5	121.3
C2-C8-C14	120.8	121.1	121.1	121.3	121.3	121.3	121.3	120.1
C8-C14-C13	120.8	119.8	119.8	119.8	120.0	120.1	120.1	117.2
C14-C13-C3	116.6	118.1	118.1	117.6	117.4	117.2	117.2	117.2
C13-N19-C16	130.4	132.0	132.0	132.3	132.3	132.1	132.2	132.1
N19-C16-S7	129.5	130.4	130.4	130.0	129.9	129.9	129.9	129.9
N19-C16-N20	112.3	112.4	112.4	112.5	112.4	112.5	112.7	112.5
S7-C16-N20	118.2	117.2	117.2	117.5	117.6	117.5	117.4	117.5
C16-N20-N21	121.1	119.3	119.3	121.3	121.4	117.8	121.7	121.5
N20-N21-C18	117.8	117.8	117.8	119.1	119.5	119.4	119.4	119.4
N21-C18-C12	127.3	125.9	125.9	126.7	126.7	126.8	126.8	126.8
N21-C18-C15	126.0	127.5	127.5	126.6	126.6	126.6	126.7	126.6
C18-C12-O9	127.1	125.6	125.6	126.4	126.5	126.5	126.6	126.5
O9-C12-N6	127.2	127.8	127.8	127.4	127.4	127.3	127.2	127.3
N6-C10-C4	128.9	129.5	129.5	128.8	128.8	128.8	128.7	128.8
C17-C15-C18	133.3	132.7	132.7	133.4	133.3	133.4	133.4	133.4
C15-C18-C12	106.6	106.5	106.5	106.7	106.6	106.6	106.5	106.6
C18-C12-N6	105.8	106.5	106.5	106.2	106.1	106.2	106.2	106.2
C12-N6-C10	111.8	110.9	110.9	111.3	111.4	111.3	111.3	111.3
N6-C10-C15	108.9	109.3	109.3	109.4	109.4	109.3	109.4	109.3
C10-C15-C17	119.8	120.6	120.6	120.1	120.1	120.0	120.0	120.0
C15-C17-C11	117.9	118.5	118.5	118.6	118.6	118.6	118.6	118.6
C17-C11-C5	121.1	120.5	120.5	120.6	120.6	120.6	120.6	120.6
C11-C5-C4	121.6	121.4	121.4	121.5	121.4	121.4	121.4	121.4
C5-C4-C10	117.4	117.8	117.8	117.4	117.4	117.4	117.4	117.4
C4-C10-C15	122.4	121.2	121.2	121.9	121.8	121.9	121.9	121.9
R <sup>2</sup>	0.979	0.979	0.989	0.984	0.982	0.979	0.979	0.990
(b) RHF								
C1-C3-F32	120.1	120.1	120.8	120.0	119.0	120.9	120.9	118.9
F32-C3-C13	116.5	116.0	120.7	117.6	117.8	117.8	117.8	117.8
C3-C13-N19	116.8	116.6	127.3	115.0	115.2	116.3	115.3	115.3
C14-C13-N19	126.6	124.6	114.7	127.5	127.4	127.4	127.4	127.4
C13-C3-C1	123.4	122.9	122.5	123.3	123.2	123.4	123.4	123.3
C3-C1-C2	118.1	118.9	119.1	118.6	118.7	118.7	118.7	118.7
C1-C2-C8	120.2	119.4	119.5	119.4	119.4	120.3	119.3	119.4
C2-C8-C14	120.8	121.1	121.1	121.3	121.3	121.3	121.3	121.3
C8-C14-C13	120.8	119.8	119.9	119.9	120.0	120.0	120.0	120.1
C14-C13-C3	116.6	117.8	118.0	117.4	117.4	117.3	117.3	117.3
C13-N19-C16	130.4	132.2	131.9	132.6	132.6	130.5	132.5	132.6
N19-C16-S7	129.5	129.6	130.5	129.2	129.1	129.1	129.1	129.1
N19-C16-N20	112.3	114.0	111.5	113.8	113.8	112.8	113.8	114.0
S7-C16-N20	118.2	116.4	118.0	117.0	117.1	117.1	117.1	116.9
C16-N20-N21	121.1	119.5	119.5	121.3	121.4	121.5	121.5	121.6
N20-N21-C18	117.8	120.1	118.1	120.7	120.8	117.7	120.7	120.7
N21-C18-C12	127.3	126.8	125.9	127.6	127.7	120.7	127.7	127.7
N21-C18-C15	126.0	127.5	127.5	126.7	126.7	126.7	126.7	126.8
C18-C12-O9	127.1	125.7	125.7	126.3	126.4	127.4	126.4	126.6
O9-C12-N6	127.2	127.9	127.8	127.5	127.5	127.4	127.4	127.2
N6-C10-C4	128.9	129.2	129.5	128.4	128.4	128.4	128.4	128.3
C17-C15-C18	133.3	132.1	132.7	132.9	132.8	133.4	132.9	132.9
C15-C18-C12	106.6	105.7	106.6	105.7	105.7	105.6	105.6	105.6
C18-C12-N6	105.8	106.4	106.5	106.2	106.1	105.8	106.1	106.2
C12-N6-C10	111.8	111.5	110.9	111.8	111.9	111.9	111.9	111.8
N6-C10-C15	108.9	109.4	109.2	109.7	109.7	108.7	109.7	109.8

C10-C15-C17	119.8	120.9	120.6	120.5	120.5	119.9	120.5	120.5
C15-C17-C11	117.9	118.4	118.5	118.4	118.5	118.5	118.5	118.5
C17-C11-C5	121.1	120.3	120.5	120.4	120.3	121.1	120.3	120.3
C11-C5-C4	121.6	121.5	121.4	121.7	121.7	121.6	121.6	121.6
C5-C4-C10	117.4	117.6	117.8	117.2	117.2	117.5	117.2	117.2
C4-C10-C15	122.4	121.4	121.2	121.9	121.8	122.4	121.9	121.9
R <sup>2</sup>	0.973	0.980	0.978	0.978	0.970	0.979	0.979	0.979

TABLE-3  
MULLIKAN AND NBO CHARGES CALCULATED WITH B3LYP AND RHF METHODS FOR I2FPTH2

Atom	B3LYP		RHF		Atom	B3LYP		RHF	
	Mullikan	NBO	Mullikan	NBO		Mullikan	NBO	Mullikan	NBO
C13	0.093	0.107	0.184	0.149	N17	-0.268	-0.373	-0.371	-0.467
C11	0.422	0.641	0.611	0.794	C18	0.229	0.277	0.378	0.459
N7	-0.480	-0.596	-0.616	-0.676	N21	-0.463	-0.576	-0.592	-0.656
C4	0.233	0.192	0.305	0.240	S20	-0.213	-0.193	-0.320	-0.327
C2	-0.040	-0.244	-0.054	-0.252	C22	0.162	0.102	0.192	0.127
C3	-0.090	-0.168	-0.071	-0.124	C25	-0.066	-0.215	-0.079	-0.198
C5	-0.101	-0.216	-0.106	-0.221	C28	-0.105	-0.196	-0.096	-0.179
C9	-0.026	-0.157	-0.032	-0.111	C30	-0.085	-0.197	-0.090	-0.179
C8	-0.134	-0.106	-0.166	-0.141	C26	-0.107	-0.264	-0.121	-0.250
O15	-0.371	-0.616	-0.476	-0.690	C24	0.211	0.408	0.305	0.443
N16	-0.237	-0.244	-0.291	-0.240	F27	-0.248	-0.362	-0.334	-0.405

TABLE-4  
FUKUI FUNCTIONS VALUES FOR I2FPTH<sub>2</sub>

HOMO		LUMO			
Atoms	6-31G(d,p)	6-311G (d,p)	Atoms	6-31G(d,p)	6-311G (d,p)
C3	3.33	4.29	C3	6.46	6.68
C4	2.66	3.47	C4	3.94	3.88
C5	1.28	1.78	N7	1.41	1.33
C8	2.62	3.53	C8	3.15	3.42
C9	1.18	1.45	C9	4.99	5.24
C13	3.93	4.92	C11	9.99	9.88
O15	2.36	2.94	C13	13.41	13.73
N16	1.2	1.59	O15	8.71	8.27
N17	5.03	6.74	N16	24.82	24.21
C18	1.16	1.71	N17	4.1	3.84
S20	49.16	47.69	C18	5.84	5.84
N21	8.35	6.31	S20	8.34	8.58
C22	3.02	2	N21	1.81	1.72
C24	3.77	2.73	—	—	—
C25	1.68	1.17	—	—	—
C28	1.95	1.46	—	—	—
C30	4.97	3.49	—	—	—

the spectra of Zn[(I2FPTH)<sub>2</sub>] complex. This is due to coordination of thione sulphur to the zinc ion. The strong band appearing at 1571 cm<sup>-1</sup> in the IR spectrum of I2FPTH<sub>2</sub> ligand shifted towards lower wave number in the spectra of Zn[(I2FPTH)<sub>2</sub>] complex. Shifting towards lower wave number is due to the coordination of azomethine nitrogen with metal ion.

**NMR studies:** Chemical shifts of the <sup>1</sup>H and <sup>13</sup>C NMR for I2FPTH<sub>2</sub> are given in Tables 6 and 7, respectively. These chemical shifts were obtained from calculations with RHF and DFT methods employing the basis sets 3-21G, 3-21G\*, 6-31G(d,p), 6-311G(d,p), 6-311+G(d,p), 6-311++G(d,p) and 6-311++G(2d,2p). <sup>1</sup>H NMR chemical shifts correlation coefficient for I2FPTH<sub>2</sub> except indole hydrogen employing the basis sets 3-21G, 3-21G\*, 6-31G(d,p), 6-311G(d,p), 6-311+G(d,p), 6-311++G(d,p) and 6-311++G(2d,2p) are 0.654, 0.864, 0.654, 0.639, 0.676, 0.684 and 0.693 for RHF method,

respectively while they are 0.852, 0.854, 0.831, 0.808, 0.825, 0.830 and 0.830 for B3LYP method, respectively. H30 and H25 chemical shifts are assigned experimentally at 11.26, 12.86 and theoretically calculated as 9.24, 11.41 by using B3LYP/6-311+G(d,p). In addition, <sup>13</sup>C NMR chemical shifts correlation coefficient for I2FPTH<sub>2</sub> employing the basis sets 3-21G, 3-21G\*, 6-31G(d,p), 6-311G(d,p), 6-311+G(d,p), 6-311++G(d,p) and 6-311++G(2d,2p) are 0.872, 0.967, 0.947, 0.946, 0.946, 0.946 and 0.953, respectively, obtained from RHF method and 0.872, 0.967, 0.947, 0.970, 0.970, 0.968 and 0.969, respectively, obtained from B3LYP method. The NMR chemical shifts employing the basis sets of 6-311G(d,p) and 6-311+G(d,p) are given in Table-8 together with experimental values for Zn[(I2FPTH)<sub>2</sub>].

Proton NMR of Zn[(I2FPTH)<sub>2</sub>] shows a characteristic indole NH signal at δ 10.67 ppm that is similar to that for the I2FPTH<sub>2</sub> ligand at δ 10.71 ppm. The characteristic proton signals

TABLE-5  
EXPERIMENTAL AND THEORETICAL FT-IR VALUES OF 4-(2-FLUOROPHENYL)-1-(2-OXOINDOLIN-3-YLIDENE)THIOSEMICARBAZONE “I2FPTH<sub>2</sub>,” AND ITS ZINC(II) COMPLEX“Zn[(I2FPTH)<sub>2</sub>]”

Ligand			Zn			
Exp.	6-311	Intensity	Exp.	6-311	Intensity	Signs
3313	3535	76	3364	3647	73	v(N7H12)
3187	3492	116	3180	3570	218	v(N21H)
3152	3438	92	—	—	—	v(N17H)
3073	3237	10	3063	3239	138	v(C25H)
—	3199	15	—	—	—	v(CH)ring C
—	3193	14	—	3204	20	v(CH)ring A
—	3191	15	—	3199	22	v(CH)ring C
—	—	—	—	3187	14	v(CH)ring C
1690	1731	274	1697	1793	577	v(C11O15), v(C13N16), δ(N17H19), δ(N7H12)
1618	1663	82	1611	1662	203	δ(N7H), v(CC)ring C
	1659	130	1595	1635	81	δ(N21H23), v(CC)ring A, δ(CH)ring A
1594	1639	135	—	—	—	v(C18N21), δ(N21H), v(CH)ring A
1571	1625	150	—	—	—	δ(N17H), v(C13N16), δ(N7H)
1538	1590	737	1505	1595	75	δ(N21H), v(C18N21), δ(CH)ring A
1530	1528	108	—	—	—	δ(N17H), δ(N21H), v(C18S20), v(CH)ring A
—	—	—	1456	1575	819	δ(N21H), v(C18N21), δ(CH)ring A
1470	1518	39	—	—	—	δ(N7H), δ(N21H), v(C18S20), v(CH)ring A, v(CH)ring C
—	—	—	1418	1514	78	δ(N21H), δ(CH)ring A
—	—	—	—	1499	136	δ(CH)ring C
1463	1508	77	—	—	—	δ(N17H), δ(N21H), δ(CH)ring A, δ(CH)ring C, v(C18S20)
1451	1495	60	—	—	—	δ(N17H), δ(CH)ring A, δ(CH)ring C
1407	1488	183	—	—	—	δ(N17H), δ(CH)ring A, δ(CH)ring C, v(C18N21)
—	1425	81	—	—	—	δ(N7H), v(C18N21), δ(CH)ring C
—	—	—	1383	1444	1287	v(N21C18N17), v(N16C13)
1344	1400	324	—	1441	2159	δ(N21H), δ(N17H), δ(N7H), v(C18N21)
—	—	—	1336	1420	157	δ(N7H), δ(CH)ring C
1320	1366	53	—	—	—	δ(N7H), δ(CH)ring C
1296	1349	34	1293	1363	194	v(CC)ring A, v(C22N21C18), δ(CH)ring C
1270	1324	48	—	—	—	δ(N17H), δ(CH)ring C, v(CC)ring C, v(N7C11)
—	—	—	1277	1357	76	δ(N7H), δ(CH)ring C
—	—	—	—	1322	40	δ(N21H), δ(CH)ring A
—	—	—	1237	1299	124	δ(N21H), δ(N7H), δ(CH)ring A, v(N17N16)
1227	1294	24	—	—	—	δ(N17H), δ(N7H), δ(CH)ring C, v(N7C11)
—	—	—	1214	1269	163	δ(CH)ring A, δ(N7H)
—	—	—	—	1251	15	δ(N7H), δ(CH)ring A, δ(CH)ring C
1207	1246	56	—	—	—	δ(N17H), δ(N7H), δ(CH)ring C
1198	1221	261	—	—	—	δ(N17H), δ(N7H), δ(CH)ring C, v(C24F27)
—	1218	130	—	—	—	δ(N17H), δ(N7H), δ(CH)ring A, v(N17C18), v(C24F27),
—	—	—	1169	1197	220	δ(CH)ring A, δ(CH)ring C, δ(N7H), δ(N21H),
1134	1192	693	—	—	—	δ(CH)ring A, δ(N21H), δ(CH)ring C, v(N17N16), δ(ringB)
1100	1179	69	—	—	—	δ(CH)ring C, δ(N7H)
—	—	—	—	1180	39	δ(CH)ring C
—	—	—	—	1177	48	δ(CH)ring A
—	—	—	1143	1167	446	δ(CH)ring A, δ(CH)ring C, δ(N7H), δ(N21H), v(N17N16),
1030	1163	147	—	—	—	δ(C25H), δ(C26H), δ(C30H), δ(N21H), δ(N17H), v(N17C18)
982	1123	12	1091	1126	99	δ(CH)ring C
945	1112	6	1041	1116	83	δ(CC)ring A, δ(N21H),
864	1056	14	—	1057	22	δ(CH)ring A,
—	—	—	1008	997	57	ω(CH)ring C
817	963	46	—	832	150	v(S20C10)
788	832	—	—	—	—	v(C24F27), δ(isatin)
—	808	—	—	—	—	ω(CH)ring C, ω(N17H), ω(C11O15)

of NH groups (H23 and H19) are seen at  $\delta$  11.26 ppm and  $\delta$  12.86 ppm, respectively. The spectra for Zn[(I2FPTH)<sub>2</sub>] shows the presence of first peak at  $\delta$  11.03 and the absence of second

peak indicating that the hydrogen is deprotonated when the ligand coordinates through S20 and N16 atoms. C9(H14) proton signal for I2FPTH<sub>2</sub> ligand seen at  $\delta$  11.26 ppm shifts

**TABLE-6**  
 **$^1\text{H}$  NMR CHEMICAL SHIFTS FOR I2FPTH<sub>2</sub> OBTAINED FROM RHF AND DFT METHODS**

I2FPTH <sub>2</sub>	Exp.	RHF					
		3-21 G(d.p)	3-21G* (d.p)	6-31 G(d.p)	6-311 G(d.p)	6-311+ G(d.p)	6-311++ G(d.p)
H14	7.40	8.40	8.11	8.34	8.25	8.48	8.49
H1	6.94	7.00	7.05	7.08	6.95	7.10	7.09
H10	7.37	7.51	7.58	7.40	7.25	7.41	7.50
H5	7.49	7.88	7.75	7.80	7.68	7.82	7.91
H29	7.70	9.92	9.69	10.03	9.85	10.00	9.97
H31	7.32	7.25	7.17	7.51	7.39	7.55	7.54
H32	7.26	7.74	7.61	7.59	7.45	7.56	7.64
H33	7.10	7.52	7.47	7.47	7.29	7.40	7.39
H23	11.26	9.00	10.23	9.15	8.81	9.24	9.27
H19	12.86	11.41	12.91	11.32	10.95	11.41	11.41
H12	10.71	5.65	6.38	6.45	6.21	6.68	6.69
R <sup>2</sup>		0.654	0.864	0.654	0.639	0.676	0.684
B3LYP							
H14	7.40	7.43	7.24	7.74	7.90	8.03	8.01
H1	6.94	6.38	6.18	6.72	6.86	6.87	6.83
H10	7.37	6.90	6.71	7.15	7.25	7.32	7.31
H5	7.49	7.08	6.89	7.32	7.42	7.51	7.49
H29	7.70	9.14	8.94	9.84	10.00	10.06	10.03
H31	7.32	6.49	6.29	7.09	7.26	7.33	7.31
H32	7.26	6.96	6.75	7.24	7.35	7.30	7.33
H33	7.10	6.82	6.61	7.13	7.19	7.16	7.31
H22	11.26	9.57	9.35	10.04	9.98	10.26	10.30
H19	12.86	12.44	12.22	12.71	12.50	12.78	12.76
H12(indole)	10.71	5.71	5.51	6.51	6.54	6.82	6.85
R <sup>2</sup>		0.852	0.854	0.831	0.808	0.825	0.830

The carbon signals at 178.7 ppm. (C=S) and (C=N) shift to 186.99 and 130.90 ppm, respectively 8.22 ppm after zinc(II) coordination.

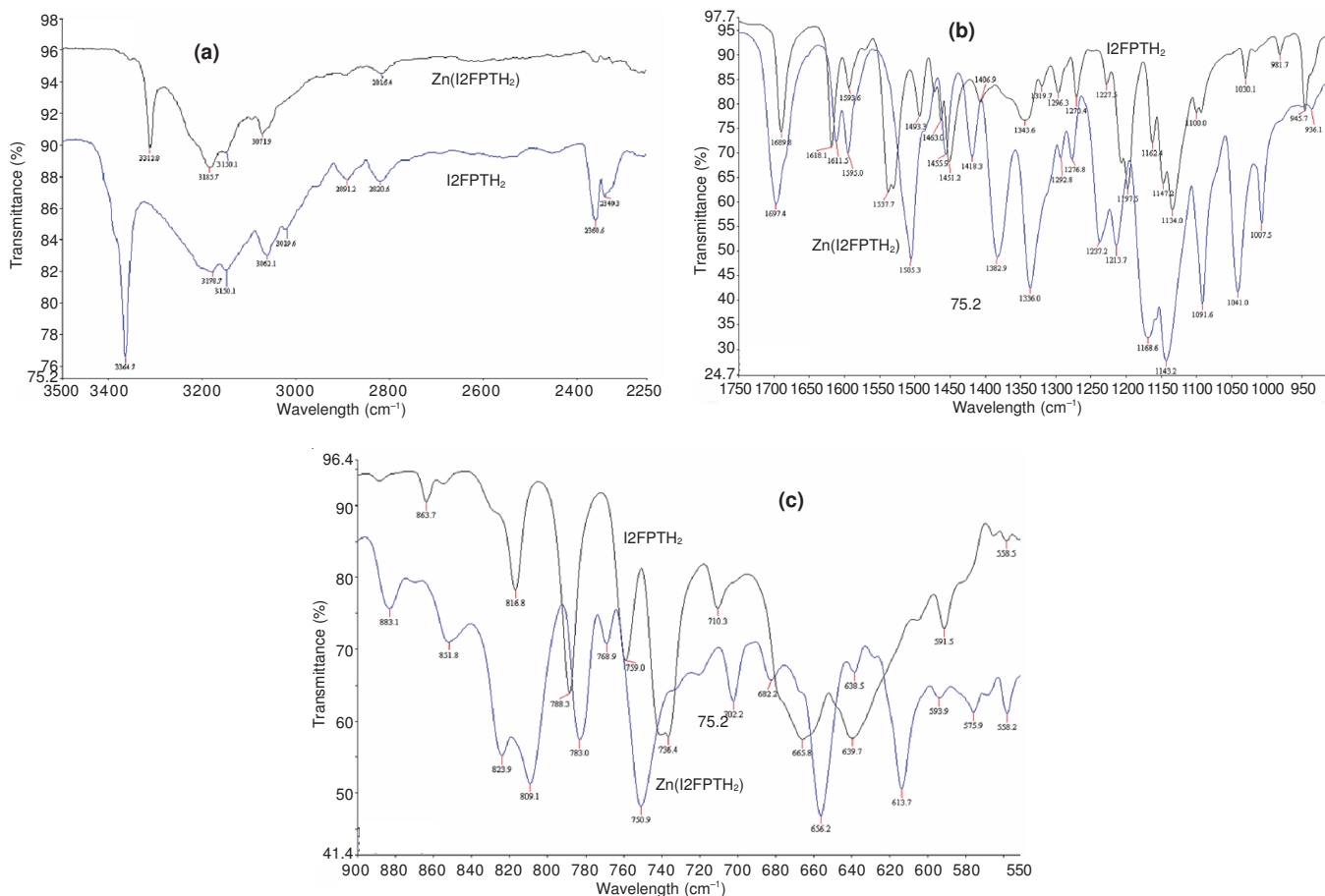


Fig. 3. (a-c) Experimental FT-IR graphics of 4-(2-fluorophenyl)-1-(2-oxoindolin-3-ylidene)thiosemicarbazone “I2FPTH<sub>2</sub>” and its zinc(II) complex “Zn(I2FPTH<sub>2</sub>)”

TABLE-7  
<sup>13</sup>C NMR CHEMICAL SHIFTS FOR I2FPTH<sub>2</sub> OBTAINED FROM RHF AND DFT METHODS

RHF							
I2FPTH <sub>2</sub>	Exp.	3-21G (d,p)	3-21G* (d,p)	6-31 G(d,p)	6-311 G(d,p)	6-311+ G(d,p)	6-311++ G(d,p)
C9	130	119	119	126	132	133	133
C5	122	115	121	121	127	128	128
C3	132	127	126	134	141	142	142
C2	116	104	109	108	114	114	113
C4	143	134	136	143	150	151	150
C8	120	110	118	117	123	124	124
C18	133	128	128	129	133	134	134
C11	163	161	160	161	166	168	168
C18	178	188	164	192	197	199	199
C22	131	122	127	127	133	134	133
C25	158	141	150	148	155	156	155
C24	123	115	116	122	128	128	127
C26	112	110	113	114	120	121	119
C28	127	119	122	124	131	132	130
C30	125	117	120	124	130	131	129
R <sup>2</sup>	—	0.872	0.967	0.947	0.946	0.946	0.953
B3LYP							
C9	129.50	108.53	107.48	116.43	126.60	126.83	126.73
C5	121.71	110.19	109.16	118.20	128.48	129.06	129.51
C3	132.01	116.11	115.03	125.01	136.09	136.62	136.57
C2	116.45	98.59	97.56	105.46	114.20	114.68	114.62
C4	143.09	126.01	124.98	136.55	148.03	148.49	148.62
C8	120.32	107.90	106.92	117.60	127.26	128.17	128.35
C13	133.19	118.10	116.96	123.64	131.59	132.59	132.36
C11	163.11	149.03	147.97	155.82	166.26	168.87	168.88
C18	178.41	160.59	158.11	169.80	180.64	182.41	182.52
C22	130.61	116.27	115.38	124.26	134.65	135.41	135.30
C25	157.74	140.15	139.11	148.48	161.87	162.28	162.61
C24	122.90	105.64	104.59	114.46	124.12	123.85	124.62
C26	111.61	102.31	101.26	109.52	119.18	119.52	119.83
C28	126.94	111.45	110.39	119.39	129.99	130.52	130.84
C30	124.87	110.35	109.25	118.67	129.14	129.32	129.46
R <sup>2</sup>	—	0.872	0.967	0.947	0.970	0.970	0.968

TABLE-8  
<sup>1</sup>H AND <sup>13</sup>C NMR CHEMICAL SHIFT FOR Zn[(I2FPTH)<sub>2</sub>]

<sup>1</sup> H							
Atom	Exp.	6-311 G(d,p)	6-311+G(d,p)	Atom	Exp	6-311 G(d,p)	6-311+G(d,p)
H14	7.70	7.73	8.60	H31	7.70	7.23	7.22
H1	7.10	6.76	6.93	H32	7.36	7.53	7.58
H10	7.26	7.21	7.25	H33	7.26	7.17	7.17
H5	7.01	6.60	6.4	H22	11.03	7.95	7.87
H29	8.00	10.35	10.54	H12	10.67	6.16	6.28
<sup>13</sup> C							
C9	—	130.08	131.47	C18	—	182.80	184.29
C5	—	126.00	127.31	C22	—	133.99	134.36
C3	—	137.79	138.42	C25	—	160.95	161.51
C2	—	112.54	112.75	C24	—	130.43	131.59
C4	—	147.39	148.14	C26	—	118.35	118.80
C8	—	124.74	126.32	C28	—	131.44	132.12
C13	—	148.69	151.23	C30	—	128.80	129.33
C11	166.79	161.72	163.97	—	—	—	—

downfield to 7.70 ppm in Zn[(I2FPTH)<sub>2</sub>] complex due to the nearby position to C=N group and may be the most affected by the Zn-N bond formation<sup>19</sup>.

**UV study:** The UV visible spectral values, excitation energies and oscillator strengths for I2FPTH<sub>2</sub> ligand were performed at the TDB3LYP levels by using 6-311G(d,p), 6-311++G(d,p) and 6-311G(d,p) basis sets for Zn[(I2FPTH)<sub>2</sub>]

complex, as shown in Table-9. The bands assigned experimentally at 256 nm were found at 256 nm with the calculation TDB3LYP/6-311G(d,p) due to transitions mainly from HOMO-2 to LUMO+1 and from HOMO to LUMO+2. HOMO-2 and HOMO consist of -7.5 % 2pz(N21)+ 7.5 % 2pz(N17)- 6.2 % 2pz(C30)+ 5.0 % 2pz(C22)- 4.5 % 3pz(C30)+ 4.5 % 2pz(C24) and + 30.9 % 3pz(S20)+ 17.9 % 4pz(S20)-

TABLE-9 UV VISIBLE SPECTRAL VALUES, EXCITATION ENERGIES AND OSCILLATOR STRENGTHS FOR I2FPTH <sub>2</sub> LIGAND AND Zn[(I2FPTH) <sub>2</sub> ] (nm)		
Experiment	I2FPTH <sub>2</sub>	
	370 nm (27027)	256 nm(39062)
6-311 G(d,p)	352[3.51(0.46) E4]	256[4.85(0.18) E10]
6-311+G(d, p)	359[3.45(0.45) E4]	267[4.64(0.16) E9]
6-311+G(d,p)	359[3.45(0.45) E4]	267[4.64(0.16) E9]
Experiment	Zn[(I2FPTH) <sub>2</sub> ]	
	435 nm	252 nm
6-311 G(d,p)	462[2.68(0.24) E5]	264[4.69(0.32) E32]
6-311+G(d, p)	479[2.59(0.25) E3]	267[4.64(0.30) E32]

5.4 % 2pz(N21)-3.4 % 2pz(N17)-2.9 % 3pz(N21)- 2.9 % 2pz(C30). LUMO+1 and LUMO+2 consist of + 14.1 % 2pz(C18)- 9.1 % 2pz(C30)- 8.3 % 2pz(C22)-7.3 % 3pz(C30)+ 6.7 % 3pz(C18)- 6.3 % 2pz(N17) and + 15.9 % 2pz(C2)+ 15.6 % 2pz(C9)+ 12.7 % 3pz(C2)+ 12.2 % 3pz(C9)+ 6.1 % 2pz(C11)- 6.0 % 2pz(C4).

The bands assigned experimentally at 370 nm were calculated with the calculation TDB3LYP/6-311G(d,p) as 352 nm due to transitions mainly due to from HOMO-3 to LUMO consisting of + 17.5 % 2pz(C24)+ 14.1 % 2pz(C28)+ 11.5 % 3pz(C28)- 11.3 % 2pz(C25)- 11.1 % 2pz(C26)- 9.1 % 3pz(C26) and + 16.5 % 2pz(N16)+ 8.3 % 3pz(N16)- 7.1 % 2pz(C13)+ 5.8 % 2pz(O15)- 5.7 % 3pz(C13)- 5.6 % 2pz(C11).

The bands of I2FPTH<sub>2</sub> ligand at 370 and 256 nm shifts to 435 and 252 nm in the spectrum of Zn[(I2FPTH)<sub>2</sub>]. This changes are due to the electron delocalization on thiosemicarbazone group upon coordination with Zn(II) ions.

## Conclusion

The optimized geometrical parameters, bond lengths and bond angles, were calculated theoretically by using the density functional and RHF methods and compared with the experimental data for studied molecule. Using of RHF method is somewhat better than the B3LYP for all calculated basis sets for the calculations of bond lengths. The highest correlation coefficient for bond lengths was 0.9745 for RHF/6-311++G(2d,2p). The agreement between the calculated and the experimental bond angles is better than for the bond lengths.

Moreover, according to results of Fukui functions values of I2FPTH<sub>2</sub>, it is found that sulphur atom contributes dominantly to the HOMO, while nitrogen 16 atom play important role for contribution to the LUMO.

The IR spectrum of I2FPTH<sub>2</sub> shows that bands at 3313 cm<sup>-1</sup> attributed to v(NH) cm<sup>-1</sup> vibration of the indole ring and thiosemicarbazone moiety. It is also concluded from IR results that a very strong band at 1690 and 1697 cm<sup>-1</sup> assigned to (C=O) stretching vibration of ligand and its Zn(II) complex. Besides, the band corresponding to the stretching vibration of the C=S group appears at 1200-1194 cm<sup>-1</sup>.

According to results of the theoretical studies of <sup>1</sup>H and <sup>13</sup>C NMR chemical shifts for I2FPTH<sub>2</sub>, since C9(H14) proton signal seen at δ 11.26 ppm shifts downfield to 7.70 ppm in Zn[(I2FPTH)<sub>2</sub>] complex due to the nearby position to C=N group, it can be said that the Zn-N bond formation effects this proton signal.

In addition, the bands assigned at 256 nm were found at 256nm with the calculation TDB3LYP/6-311G(d,p) due to transitions mainly from HOMO-2 to LUMO+1 and from HOMO to LUMO+2 due to the results of calculation of UV visible spectral values, excitation energies and oscillator strengths for I2FPTH<sub>2</sub> ligand.

In this study, results obtained theoretically are sensibly consistent with the results of experimental study.

## ACKNOWLEDGEMENTS

The financial support for this study was provided by the BAP Fund (Project Number: FEB 2010/37)

## REFERENCES

1. S.K. Sridhar and R. Atmakuru, *Indian Drugs*, **38**, 174 (2001).
2. S.N. Pandeya and D. Sriram, *Acta Pharm. Turc.*, **40**, 33 (1998).
3. R.S. Varma and W.L. Nobles, *J. Pharm. Sci.*, **64**, 881 (1975).
4. S.N. Pandeya, P. Yogeeshwari, D. Sriram, E. De Clercq, C. Panneccouque and M. Witvrouw, *Cancer Therapy*, **45**, 192 (1999).
5. C. David, T. Marie and G. Roussel, U.S. Patent, 5,498,716 (1996); *Chem. Abstr.*, **124**, 343271 (1996).
6. S.N. Pandeya, D. Sriram, G. Nath and Clercq E. De, *Pharm. Acta Helv.*, **74**, 11 (1999).
7. S.A. Imam and R.S. Varma, *Experientia*, **31**, 1287 (1975).
8. N. Karali, A. Gürsoy, F. Kandemirli, N. Shvets, F.B. Kaynak, S. Özbeý, V. Kovalishyn and A. Dimoglo, *Bioorg. Med. Chem.*, **15**, 5888 (2007).
9. G. Cerchiaro and A.C. Ferreira, *J. Braz. Chem. Soc.*, **17**, 1473 (2006).
10. S. Gunesdogdu-Sagdinc, B. Köksoy, F. Kandemirli and S.H. Bayari, *J. Mol. Struct.*, **917**, 63 (2009).
11. F. Kandemirli, T. Arslan, N. Karadayi, E.E. Ebenso and B. Köksoy, *J. Mol. Struct.*, **938**, 89 (2009).
12. F. Kandemirli, T. Arslan, B. Koksoy and M. Yilmaz, *J. Chem. Soc. Pak.*, **31**, 498 (2009).
13. F. Kandemirli, B. Koksoy, T. Arslan, S. Sagdinc and H. Berber, *J. Mol. Struct.*, **921**, 172 (2009).
14. H. Pervez, M. Yaqub, M. Ramzan, M.S. Iqbal and M.N. Tahir, *Acta Cryst.*, **E66**, 01405 (2010).
15. S.G. Sagdinc, F. Kandemirli, B. Köksoy and S.H. Bayari, *Phosphorus Sulfur Silicon Rel. Elem.*, **187**, 1243 (2012).
16. M.J. Frisch, G.W. Trucks, H.B. Schlegel, G.E. Scuseria, M.A. Robb, J.R. Cheeseman, G. Scalmani, V. Barone, B. Mennucci, G.A. Petersson, H. Nakatsuji, M. Caricato, X. Li, H.P. Hratchian, A.F. Izmaylov, J. Bloino, G. Zheng, J.L. Sonnenberg, M. Hada, M. Ehara, K. Toyota, R. Fukuda, J. Hasegawa, M. Ishida, T. Nakajima, Y. Honda, O. Kitao, H. Nakai, T. Vreven, J.A. Montgomery Jr., J.E. Peralta, F. Ogliaro, M. Bearpark, J.J. Heyd, E. Brothers, K.N. Kudin, V.N. Staroverov, T. Keith, R. Kobayashi, J. Normand, K. Raghavachari, A. Rendell, J.C. Burant, S.S. Iyengar, J. Tomasi, M. Cossi, N. Rega, J.M. Millam, M. Klene, J.E. Knox, J.B. Cross, V. Bakken, C. Adamo, J. Jaramillo, R. Gomperts, R.E. Stratmann, O. Yazyev, A.J. Austin, R. Cammi, C. Pomelli, J.W. Ochterski, R.L. Martin, K. Morokuma, V.G. Zakrzewski, G.A. Voth, P. Salvador, J.J. Dannenberg, S. Dapprich, A.D. Daniels, O. Farkas, J.B. Foresman, J.V. Ortiz, J. Cioslowski and D.J. Fox, Gaussian 09, Revision B. 01, Gaussian, Inc., Wallingford CT (2010).
17. S.I. Gorelsky, AOMix: Program for Molecular Orbital Analysis; University of Ottawa, (2009); <http://www.sg-chem.net/>
18. S.I. Gorelsky and A.B.P. Lever, *J. Organomet. Chem.*, **635**, 187 (2001).
19. N.T. Akinchan, P.M. Drozdzewski and W. Holzer, *J. Mol. Struct.*, **641**, 17 (2002).
20. A.M. Asiri, A. Asiri and S.A. Khan, *Molecules*, **15**, 4784 (2010).